Bioadhesive supramolecular hydrogel from unprotected, short D,L-peptides with Phe-Phe and Leu-Asp-Val motifs

Maria Cristina Cringoli,a Chiara Romano,a Evelina Parisi,a Lynne J. Waddington,b Michele Melchionna,a Sabrina Semeraro,a Rita De Zorzi,a Mikaela Grönholm*c and Silvia Marchesan*a

The uncapped tripeptide DPhe-Phe-Leu acts as self-assembly template to yield supramolecular hydrogel biomaterials. As an example, self-assembling DPhe-Phe-Leu-Asp-Val contains the LDV bioadhesive motif for β1 integrin activation. Hydrogels made of the two peptides successfully mimic fibronectin of the extracellular matrix and lead to high cell viability, adhesion, and spreading.

Adhesion to the extracellular cell matrix (ECM) is crucial for cell survival.1 The ECM displays a complex structure, thus simple peptides are convenient alternatives to induce cell attachment onto biomaterials.2-5 Despite several years of research, most studies rely on one ECM-derived motif, i.e., Arg-Gly-Asp or RGD, which activates integrin proteins6 leading to cell adhesion.7, 8 This approach was successfully applied to gels of short peptides with aromatic N-caps (e.g., fluorenylmethyloxycarbonyl or Fmoc, naphthalene or Nap derivatives) as self-assembly templates.9-11 However, concerns exist over their biocompatibility.12-16 Supramolecular hydrogels from unprotected short peptides could be an attractive alternative, yet their assembly is far more difficult to predict.17-19 Thus, there is scope to investigate the largely unexplored chemical space of uncapped short peptides and bioadhesive motifs beyond RGD. Rational design of simple gelators could open new avenues for biomaterials with precise chemical definition.

In this work, we designed a bioadhesive hydrogel based on uncapped short peptides to fill this gap. Phe-Phe forms fibrils20 or metastable hydrogels.21, 22 Addition of Leu yields stable hydrogels at physiological conditions and without organic solvents, as long as the sequence contains D- and L-amino acids to favour an amphipathic supramolecular structure, as in DLeu-Phe-Phe, Phe-DLeu-Phe, or their enantiomers).23, 24 Thus, the unreported sequence DPhe-Phe-Leu (1 in Scheme 1) was designed for self-assembly, with the Leu strategic position at the C-terminus. In this way, a simple addition of just two amino acids yields DPhe-Phe-Leu-Asp-Val (2 in Scheme 1), whereby the structural scaffold is fused with the bioactive motif Leu-Asp-Val (LDV).25 This fibronectin-derived motif is known to activate β1 integrins leading to cell adhesion, also in nanostructured materials.26 Applications range from anti-inflammatory to anti-metastatic activities.27, 28 The LDV motif has been only recently applied to polymer, not supramolecular, hydrogels.29

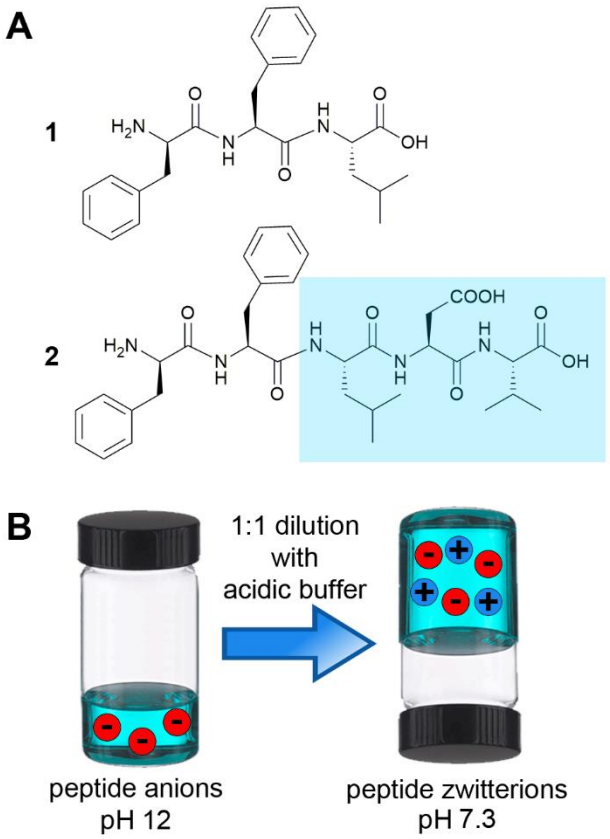

Scheme 1. A) Chemical structures of DPhe-Phe-Leu (1) and DPhe-Phe-Leu-Asp-Val (2) with the bioadhesive LDV motif (light blue square). B) Schematic of the gelation protocol.

Following a pH trigger as shown in Scheme 1, DPhe-Phe-Leu (1) gelled phosphate buffer at pH 7.3 with a minimum gelling concentration (MGC) of 5 mM (0.2 wt.%) to yield a dense network of fibril bundles with variable helical pitch as revealed by TEM, cryo-TEM and AFM (Fig. 1). Nucleation areas were composed of short, individual fibrils (5.3 ± 1.4 nm wide, n =100) entangling into nuclei (Fig. 1A), from which fragments of bundles emerged and eventually fused into micron-long fibers (Fig. 1B-C). The fibrillar network (Fig. 1D) contained twisted bundles (Fig. 1E-F) that AFM confirmed to be right-handed (Fig. 1G and ESI). The viscoelastic properties of the system were assessed by rheology (Fig. 1H-I and ESI). Time sweeps (Fig. 1H) confirmed rapid gelation kinetics with the elastic modulus G’ higher than the viscous modulus G’’ as expected for gels. The hydrogel displayed a high resistance against stress, with a gel-to-sol transition occurring at nearly 100 Pa (Fig. 1I).

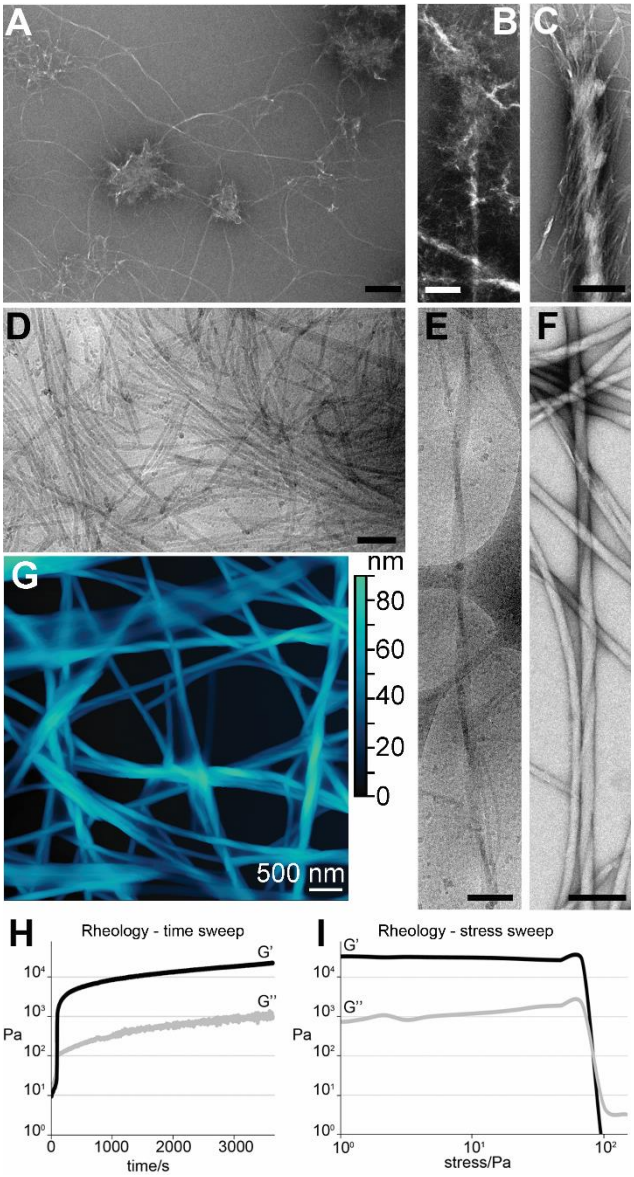

Fig. 1. A-C) TEM images of DPhe-Phe-Leu (1) nucleation with short fibrils merging into bundles. D) cryoTEM image of 1 fibril network. E) cryoTEM and (F) TEM images of 1 twisted bundles. Scale bars = 200 nm. G) AFM of 1 revealed right-handed twists. Rheology time (H) and stress (I) sweeps of 1.

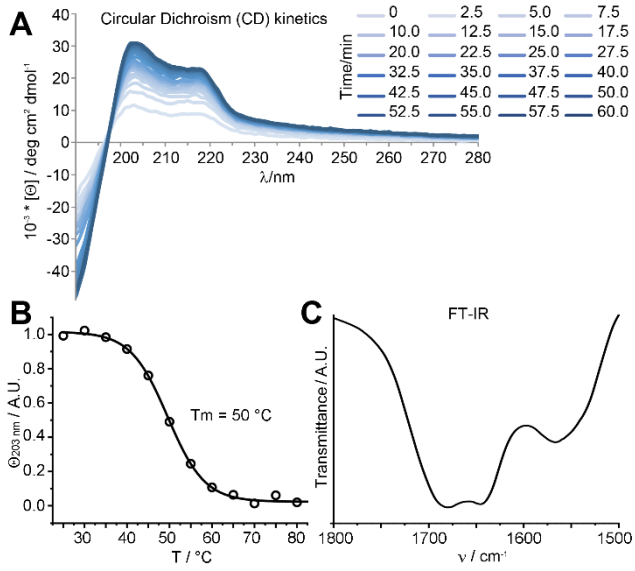

Fig. 2. A) CD spectra of DPhe-Phe-Leu (1) over 1 h of assembly. B) CD signal of 1 over a heating ramp revealed a Tm of 50 °C. C) Amide I region of FT-IR of 1.

The secondary structure was investigated by circular dichroism (CD) and FT-IR spectroscopy, as shown in Fig. 2 and ESI. CD spectra of the precursor solution at pH~12 did not change over time (see ESI), while at pH 7.3 they evolved with assembly, and were characterised by two maxima at 203 and 219 nm (Fig. 2A), similarly to self-assembling D,L-tripeptides with a kinked backbone conformation.18 Upon heating, the CD signature returned to the disassembled state with a Tm = 50 °C (Fig. 2B).30 Visual observations confirmed hydrogel melting at 52 ± 2 °C. The amide I region of the FT-IR spectrum revealed two peaks at 1641 and 1689 cm.1 compatible with β-structures and turns (Fig. 2C). The hydrogel was positive to the Thioflavin T assay, a common test for amyloid structures based on β-sheets (see ESI).31

Having identified a suitable hydrogel scaffold, we prepared DPhe-Phe-Leu-Asp-Val (2) for bioadhesion. Single-crystal XRD analysis (see ESI) revealed an antiparallel β-sheet conformation, held together by an extended network of hydrogen bonding between the amide groups, and ionic interactions between termini. Adjacent stacks interact via a hydrogen bond between the C–termini (Fig. S25A). The two Phe side chains, being adjacent and in opposite stereoconfiguration, lie on the same side of the stacked peptide backbones (Fig. S25B). This is the first XRD crystal structure of the bioactive LDV motif in a linear peptide, while the structure of this motif on the fibronectin protein, or a fragment thereof, is not yet available. The peptide was tested for cell adhesion at different concentrations, and it proved to be bioactive already at 0.5 mM (see ESI). DPhe-Phe-Leu-Asp-Val (2) gelled phosphate buffer at concentrations ≥ 50 mM, which were high for a convenient biomaterial scaffold.

Mixtures of the tripeptide 1 and the pentapeptide 2 yielded hydrogels when used in the ratio of 4:1 or higher (e.g., 10:1.5, 12:3, or 15:3 mM). High concentrations of 1 lead to more durable hydrogels in cell culture conditions, while low concentrations of 2 are preferable for a cost-effective biomaterial. Therefore, amongst the various concentrations

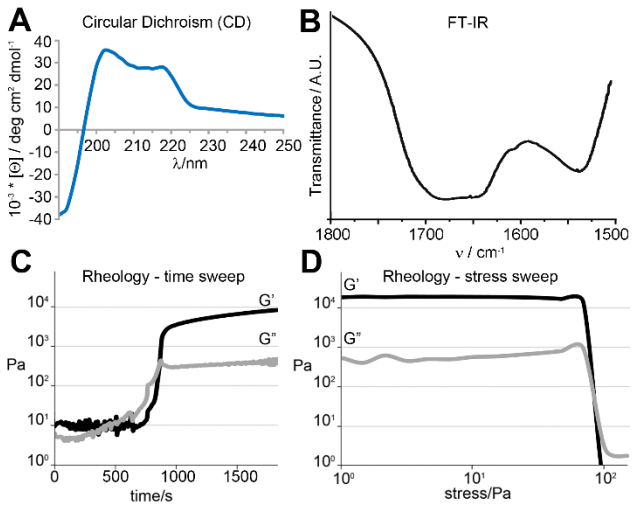

Fig. 3. Two-component gel (1 + 2).Circular dichroism (A) and FT-IR (B) spectra after 1 h of self-assembly. Rheometry time sweep (C) and stress sweep after 1 h of assembly (D).

tested (see ESI), the most advantageous was 15 mM of 1 with 1.5 mM of 2 (10:1 ratio). At these conditions, presence of the pentapeptide 2 did not significantly alter the spectroscopic properties of the hydrogel formed by 1, as shown by CD and FT-IR spectra (see Fig. 3A-B). Rheology showed that presence of 2 led to slower gelation kinetics, while the hydrogel maintained a good resistance to stress (see Fig. 3C-D and ESI).

TEM and AFM confirmed fibril morphology was retained, and also the right-handed twists, though less bundling occurred, leading to a more uniform fibril network (Fig. 4 and ESI).

Cells displayed high viability in all cases, but cell spreading occurred only in the presence of the bioactive peptide 2 (Fig. 5 and ESI). Cells were viable also within the tripeptide 1 hydrogel (Fig. 5A, centre), where they retained a round morphology. In the presence of 2 (Fig. 5A-B, left, and Fig. 5C), cells adhered and spread to a greater extent than in the hydrogel of 1 (Fig. 5A-B, centre, and Fig. 5C) or the control (Fig. 5A-B, right, and Fig. 5C). Addition of integrin β1 blocking-antibody inhibited cell adhesion (Fig. 5C), thus confirming integrin engagement. Cell adhesive response to 2 was enhanced by Mn++ (Fig. 5C), a known integrin co-activator,6 from which we inferred successful ECM biomimicry by the LDV motif of 2, leading to cell adhesion.

Conclusions

We report DPhe-Phe-Leu (1) as an unprotected tripeptide able to self-assemble into right-handed twisted fibers that yield stable hydrogels at physiological conditions. Spectroscopic analysis confirmed a β-structure compatible with a kinked backbone. Importantly, the motif could be extended by two amino acids to yield DPhe-Phe-Leu-Asp-Val (2), which is a minimalistic bioadhesive peptide scaffold capable of ECM mimicry. Single-crystal XRD data confirmed antiparallel β-sheets for 2. Hydrogels formed by both peptides activated β1 integrin proteins and led to cell adhesion and spreading, and overall high cell viability. To our knowledge, this is the first report of a bioactive and self-assembling short peptide that mimics an ECM protein and forms a bioadhesive hydrogel without the need for end-caps to template self-assembly. We think this work is a useful addition to the range of applications of uncapped, short D,L-peptide biomaterials.32-34 Importantly, it provides new principles for the rational design of bioactive motifs that go beyond existing strategies in supramolecular hydrogels.

Acknowledgements

We acknowledge funding from the Italian Ministry of University and Research (SIR grant RBSI14A7PL to SM). This work was supported by a STSM Grant (to EP) from COST Action CA15216 - European Network of Bioadhesion Expertise: Fundamental Knowledge to Inspire Advanced Bonding Technologies. MG acknowledges funding from the Magnus Ehrnrooth Foundation (Finland). XRD data were acquired at the XRD1 line at Elettra Synchrotron in Trieste (Italy).

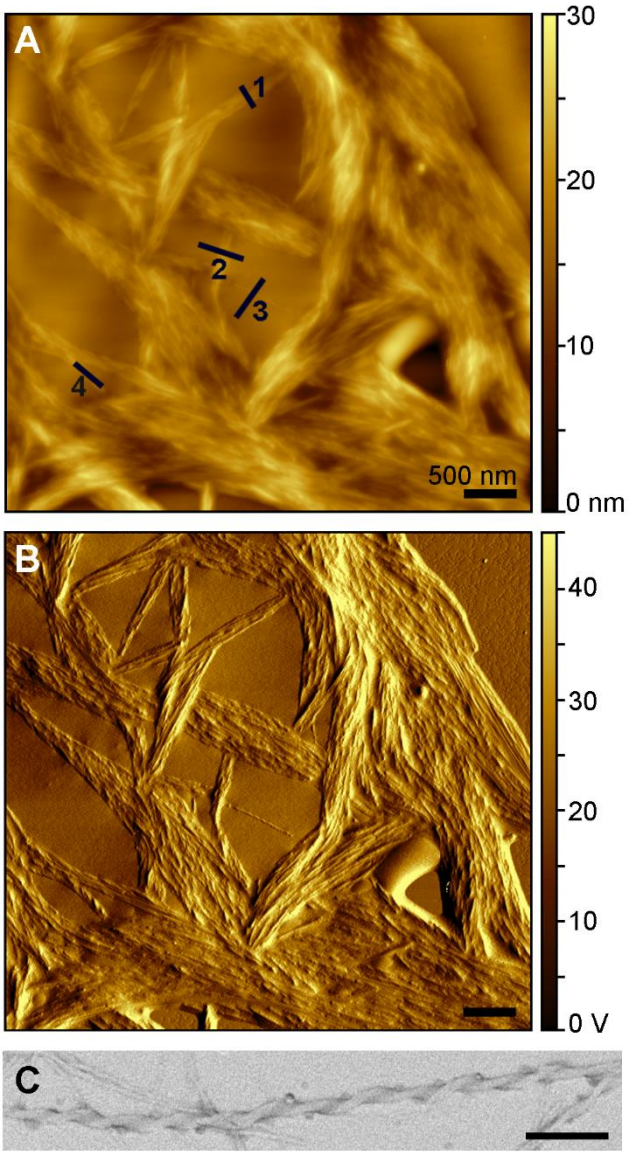

Fig. 4. Microscopy images of the two-component gel (1 + 2). AFM height (A) and amplitude (B) images. Profile scans 1-4 in (A) revealed 5.1 ± 0.9 nm-high fibrils (see ESI). C) TEM image of a twisted bundle. Scalebar = 200 nm.

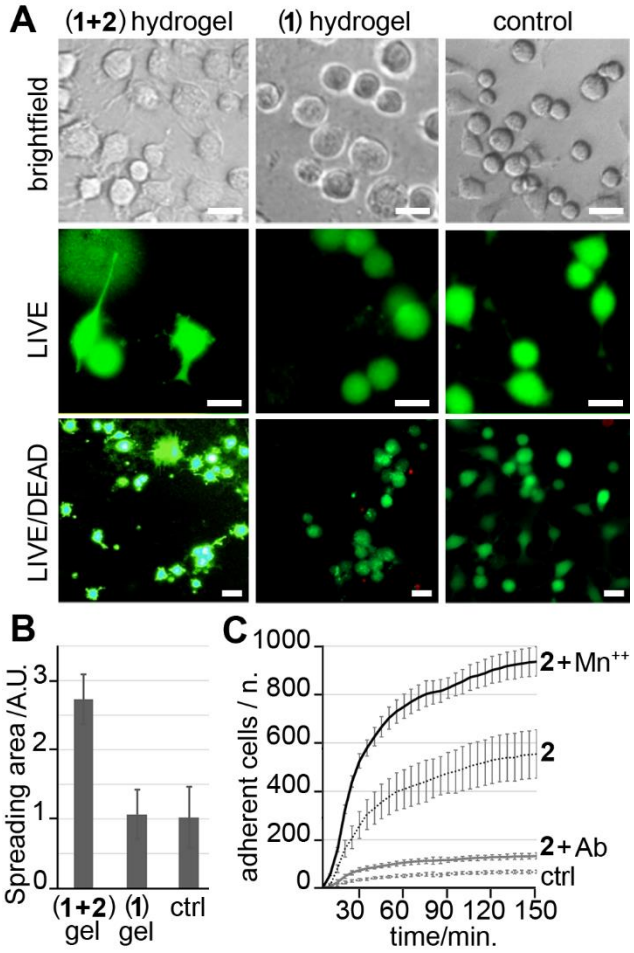

Fig. 5. A) Brightfield (top row) and fluorescence microscopy images (scale bars = 20 μm) of fibroblasts grown on and in the gels of 1 + 2 (left), 1 (centre), or on albumin control (right) for 48h reveal viable cells (green) that spread especially in the presence of 2 (left). B) Quantification of average cell area confirmed spreading due to adhesion to 2 (left). C) iCELLigence assay showed cell adhesion in response to 2 was increased by Mn++ and inhibited by β1 integrin-blocking antibody (Ab), confirming ECM biomimicry.

Conflicts of interest

There are no conflicts to declare.

References

1. A. D. Theocharis, S. S. Skandalis, C. Gialeli and N. K. Karamanos, Adv. Drug Deliv. Rev., 2016, 97, 4-27.

2. X.-Q. Dou and C.-L. Feng, Adv. Mater., 2017, 29, 1604062.

3. M. Amit, S. Yuran, E. Gazit, M. Reches and N. Ashkenasy, Adv. Mater., 2018, 30, e1707083.

4. A. Méndez-Ardoy, J. R. Granja and J. Montenegro, Nanoscale Horiz., 2018, 3, 391-396.

5. M. Aviv, M. Halperin-Sternfeld, I. Grigoriants, L. Buzhansky, I. Mironi-Harpaz, D. Seliktar, S. Einav, Z. Nevo and L. Adler-Abramovich, ACS Appl. Mater. Interfaces, 2018, 10, 41883-41891.

6. C. G. Gahmberg, S. C. Fagerholm, S. M. Nurmi, T. Chavakis, S. Marchesan and M. Grönholm, Biochim. Biophys. Acta, 2009, 1790, 431-444.

7. Y. Qian, X. Zhao, Q. Han, W. Chen, H. Li and W. Yuan, Nat. Commun., 2018, 9, 323.

8. A. Farrukh, J. I. Paez and A. del Campo, Adv. Funct. Mater., 2019, 29, 1807734.

9. G. Cheng, V. Castelletto, R. R. Jones, C. J. Connon and I. W. Hamley, Soft Matter, 2011, 7, 1326-1333.

10. V. Castelletto, I. W. Hamley, C. Stain and C. Connon, Langmuir, 2012, 28, 12575-12580.

11. L. Zhu, K. Wang, T. Ma, L. Huang, B. Xia, S. Zhu, Y. Yang, Z. Liu, X. Quan, K. Luo, D. Kong, J. Huang and Z. Luo, Adv. Healthc. Mater., 2017, 6, 1600860.

12. J. P. Wojciechowski, A. D. Martin, A. F. Mason, C. M. Fife, S. M. Sagnella, M. Kavallaris and P. Thordarson, ChemPlusChem, 2017, 82, 383-389.

13. J. Shi and B. Xu, Nano Today, 2015, 10, 615-630.

14. W. T. Truong, Y. Su, D. Gloria, F. Braet and P. Thordarson, Biomater. Sci., 2015, 3, 298-307.

15. R. Orbach, L. Adler-Abramovich, S. Zigerson, I. Mironi-Harpaz, D. Seliktar and E. Gazit, Biomacromolecules, 2009, 10, 2646-2651.

16. H. Wang, C. Yang, M. Tan, L. Wang, D. Kong and Z. Yang, Soft Matter, 2011, 7, 3897-3905.

17. P. W. Frederix, G. G. Scott, Y. M. Abul-Haija, D. Kalafatovic, C. G. Pappas, N. Javid, N. T. Hunt, R. V. Ulijn and T. Tuttle, Nat. Chem., 2015, 7, 30-37.

18. A. M. Garcia, D. Iglesias, E. Parisi, K. E. Styan, L. J. Waddington, C. Deganutti, R. De Zorzi, M. Grassi, M. Melchionna, A. V. Vargiu and S. Marchesan, Chem, 2018, 4, 1862-1876.

19. K. H. Chan, W. H. Lee, M. Ni, Y. Loo and C. A. E. Hauser, Sci. Rep., 2018, 8, 17127.

20. M. Reches and E. Gazit, Science, 2003, 300, 625-627.

21. M. P. Conte, N. Singh, I. R. Sasselli, B. Escuder and R. V. Ulijn, Chem. Commun., 2016, 52, 13889-13892.

22. M. Kurbasic, S. Semeraro, A. M. Garcia, S. Kralj, E. Parisi, C. Deganutti, R. De Zorzi and S. Marchesan, Synthesis, 2019, 51, 2829-2838.

23. A. V. Vargiu, D. Iglesias, K. E. Styan, L. J. Waddington, C. D. Easton and S. Marchesan, Chem. Commun., 2016, 52, 5912-5915.

24. D. Iglesias, M. Melle-Franco, M. Kurbasic, M. Melchionna, M. Abrami, M. Grassi, M. Prato and S. Marchesan, ACS Nano, 2018, 12, 5530-5538.

25. P. Ung and D. A. Winkler, J. Med. Chem., 2011, 54, 1111-1125.

26. R. De Marco, A. Greco, N. Calonghi, S. D. Dattoli, M. Baiula, S. Spampinato, P. Picchetti, L. De Cola, M. Anselmi, F. Cipriani and L. Gentilucci, Biopolymers, 2017, 110, e23081.

27. Y. Kaneda, Y. Yamamoto, N. Okada, Y. Tsutsuml, S. Nakagawa, M. Kakiuch, M. Maeda, K. Kawasaki and T. Mayumi, Anti-cancer drugs, 1997, 8, 702-707.

28. J. Singh, S. Adams, M. B. Carter, H. Cuervo, W. C. Lee, R. R. Lobb, R. B. Pepinsky, R. Petter and D. Scott, Curr. Top. Med. Chem., 2004, 4, 1497-1507.

29. J. Guasch, C. A. Muth, J. Diemer, H. Riahinezhad and J. P. Spatz, Nano Lett., 2017, 17, 6110-6116.

30. A. J. Miles and B. A. Wallace, Protein Sci., 2018, 27, 1717-1722.

31. N. Amdursky, Y. Erez and D. Huppert, Acc. Chem. Res., 2012, 45, 1548-1557.

32. E. Parisi, A. M. Garcia, D. Marson, P. Posocco and S. Marchesan, Gels, 2019, 5.

33. A. M. Garcia, M. Kurbasic, S. Kralj, M. Melchionna and S. Marchesan, Chem. Commun., 2017, 53, 8110-8113.

34. M. C. Cringoli, O. Bellotto, R. De Zorzi, A. V. Vargiu and S. Marchesan, Synlett, doi: 10.1055/s-0039-1690776.